

# The relevance of ocean surface current in the ECMWF analysis and forecast system

Hans Hersbach and Jean-Raymond Bidlot

*ECMWF, Shinfield Park, Reading  
RG2 9AX, United Kingdom  
hans.hersbach@ecmwf.int*

## ABSTRACT

This document describes a preliminary adaptation of the integrated forecast system at ECMWF to incorporate ocean surface currents from an external source. An impact study is performed in a data-assimilation environment, which allows for both a proper adjustment of the atmospheric boundary condition and a suitable adaptation of the ingestion of observations that are sensitive to the ocean surface. It is found that the effect on surface stress is only about half of what would have been intuitively obtained by subtraction of the ocean current from the surface wind of a system in which no account for ocean current is given. As a result, compared to the intuitive approach, the effect on wind-generated ocean waves is found to be reduced.

## 1 Introduction

The European Centre for Medium-Range Weather Forecasts (ECMWF) has a coupled ocean-atmosphere system for seasonal and monthly forecasting (Vitart *et al.*, 2008). The seasonal system is fully coupled. The monthly forecasts are at present only coupled from day 10 onwards (which runs at a lower resolution). Moreover, in contrast to the seasonal system, that coupling does not include ocean currents.

At first sight, the importance of ocean currents seems minor. The strength of typical ocean currents is in the order of a few tenths of  $\text{ms}^{-1}$ , which is small compared to typical surface wind speed of around  $8 \text{ ms}^{-1}$ . Nevertheless, in tropical areas the ratio between the two can be  $1 \text{ ms}^{-1}$  versus  $5 \text{ ms}^{-1}$ . For ocean-wave forecasting there may be a noticeable effect. Tropical ocean currents can deflect swell, which affect the propagation over the length scale of an ocean basin of 10,000km. Wave-current interactions in western boundary currents, such as the Gulf Stream, are well known.

At ECMWF, work has recently started to include the effect of ocean current on the ECMWF atmosphere and ocean-wave model component for the medium range. Although the technical development in the ECMWF integrated forecast system (IFS) has in principle been completed, it should be stressed that at this stage no proper assessment has been made. The results described in this presentation should therefore be interpreted as preliminary. The focus will be on ocean waves and surface wind.

In Section 2, it is described how the boundary condition of an atmospheric model is adapted to include ocean surface current. Some simple considerations are presented on how an ocean current is expected to change the air flow near the surface. Section 3 handles the incorporation of ocean current in the ECMWF ocean-wave model WAM. Results of a few hindcast runs are presented in Section 4. Section 5 deals with necessary changes in the assimilation component of the ECMWF model. In section 6 an impact study of the coupled wave-atmosphere system is described. The document ends with a discussion in Section 7.

## 2 Inclusion of ocean current in the atmospheric boundary layer

In principle the inclusion of an ocean surface current in the atmospheric component is straightforward. Let the flow with respect to a coordinate frame that is fixed with respect to the Earth be denoted by  $\vec{u}_{\text{abs}}$ . This is the usual frame in which numerical weather models, including ECMWF, are defined. All what is required to include surface current is that the no-slip condition at the surface demands that the (absolute) flow at height  $z = 0$  equals the ocean current  $\vec{u}_{\text{oc}}$ , rather than being zero:

$$\vec{u}_{\text{abs}}(z = 0) = \vec{u}_{\text{oc}}. \quad (1)$$

In the ECMWF operational integrated forecast system (IFS), the lowest model level (out of 91 levels) is designed to be close to a height of 10m. It is assumed that between this layer and the surface the constant (turbulent) stress assumption is valid, using a form of Monin-Obukhov stability theory. For a certain value of stress  $\tau = \rho_a u_* \vec{u}_*$ , where  $\rho_a$  is the air density,  $\vec{u}_*$  the friction velocity and  $u_*$  its magnitude, the following vertical equation, together with boundary condition (1) is to be satisfied:

$$\frac{\partial \vec{u}_{\text{abs}}}{\partial z} = \frac{\vec{u}_*}{\kappa(z + z_0)} \Phi_M \left( \frac{z + z_0}{L} \right). \quad (2)$$

Here  $\kappa = 0.4$  is the von Kármán constant,  $\Phi_M$  is a stability-dependent gradient function and  $L$  is the Obukhov length. Detailed definitions on these quantities may be found in Part IV.3 of the [IFS-documentation \(2006\)](#). The roughness length  $z_0$  depends for light wind on the kinematic viscosity  $\nu$  ( $1.5 \times 10^{-5} \text{ m}^2 \text{s}^{-1}$ ) and on a Charnock relation for strong wind as:

$$z_0 = \alpha_M \frac{\nu}{u_*} + \alpha_{\text{ch}} \frac{u_*^2}{g}. \quad (3)$$

Here  $\alpha_M = 0.11$ ,  $g = 9.81 \text{ ms}^{-2}$  is the gravitational acceleration, and  $\alpha_{\text{ch}}$  depends on the sea state, and is on average 0.018. Typical values for  $z_0$  are within the range from 0.01 mm to 1 mm, i.e., the sea surface is very smooth. Integration of (1-3) in the ECMWF model, which includes the determination of the value of stress, depends on the details of the flow higher up in the atmosphere.

Given a solution for  $\vec{u}_{\text{abs}}$ , define  $\vec{u}_{\text{rel}}$  as the flow relative to a frame moving with the ocean current:

$$\vec{u}_{\text{abs}}(z) = \vec{u}_{\text{rel}}(z) + \vec{u}_{\text{oc}}. \quad (4)$$

This relative flow then also satisfies (2), but with the more familiar boundary condition:

$$\vec{u}_{\text{rel}}(0) = 0. \quad (5)$$

The formal solution of (2, 5) is given by:

$$\vec{u}_{\text{rel}}(z) = \frac{\vec{u}_*}{\kappa} \left\{ \ln \left( \frac{z + z_0}{z_0} \right) - \Psi_M \left( \frac{z + z_0}{L} \right) + \Psi_M \left( \frac{z_0}{L} \right) \right\}, \quad (6)$$

where  $\Phi_M(\eta) = 1 - \eta \Psi'_M(\eta)$ . Therefore, it is the relative flow, rather than the absolute flow that is connected to the surface stress. Also, the surface drag  $C_D$  connects the stress with  $\vec{u}_{\text{rel}}(10 \text{ m})$ , rather than  $\vec{u}_{\text{abs}}(10 \text{ m})$ :

$$\tau / \rho_a = C_D \vec{u}_{\text{rel}}^2(10 \text{ m}). \quad (7)$$

Among other quantities, it is the stress that provides the communication of the atmosphere with other components. This is for instance the case for the growth of ocean (surface) waves.

The question arises how the presence of an ocean current will affect the flow. The answer depends on the relative importance between the boundary conditions at the surface and higher up in the atmosphere. Let the wind profile in the absence of ocean currents be given by  $\vec{u}_{\text{nocur}}$ . In this case  $\vec{u}_{\text{nocur}}$  is equal to both the absolute and relative flow. In Figure 1 an example of a wind profile in a neutral boundary layer with a friction velocity

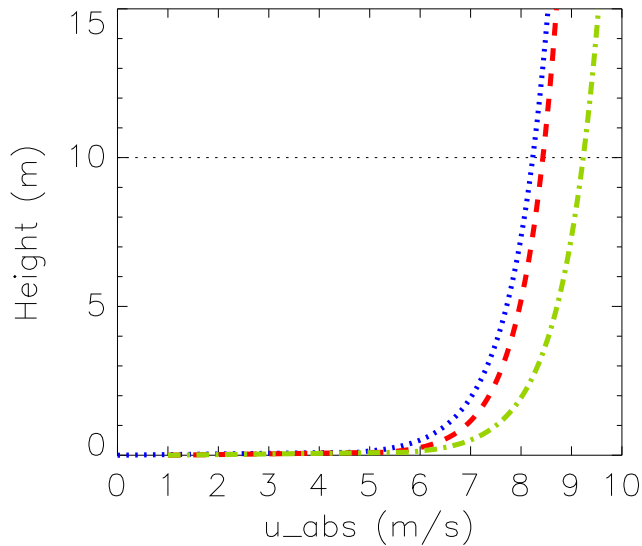


*Figure 1: Logarithmic wind profiles near the ocean surface in an absolute frame. The blue dotted profile is for  $u_* = 0.3 \text{ ms}^{-1}$  without ocean current. The green dash-dotted profile represents the situation of an ocean current of  $1 \text{ ms}^{-1}$  aligned with the wind direction and where the stress has been fixed, and the red dashed profile for a similar situation, but where the wind speed at a height of 100 m has been fixed.*

of  $0.3 \text{ ms}^{-1}$  is presented by a blue dotted line. In this case  $\Psi_M = 0$ , so (6) follows the well-known logarithmic profile. This choice corresponds to  $z_0 = 0.17 \text{ mm}$  and  $u_{\text{nocur}}(10 \text{ m}) = 8.24 \text{ ms}^{-1}$ .

Assuming that the boundary condition at the surface would dominate conditions higher up in the atmosphere would imply that the surface stress remains unchanged. Since stress is related to the relative wind, profile (6) would not be altered. The entire absolute wind profile (including higher up in the atmosphere) would be shifted:

$$\vec{u}_{\text{abs}}(z) \sim \vec{u}_{\text{nocur}}(z) + \vec{u}_{\text{oc}}, \quad \vec{u}_{\text{rel}}(z) \sim \vec{u}_{\text{nocur}}(z). \quad (8)$$

This is in principle a viable solution, since  $\vec{u}_{\text{rel}}$  satisfies (2, 3, 5). Only the boundary condition higher up is to be shifted by  $\vec{u}_{\text{oc}}$ . In Figure 1  $\vec{u}_{\text{abs}}$  is displayed by the green dot-dashed curve for the situation that there is an ocean current of  $1 \text{ ms}^{-1}$  in the direction of surface wind. Roughness length and friction velocity are unchanged,  $u_{\text{abs}}(10 \text{ m})$  is enhanced by  $1 \text{ ms}^{-1}$  to  $9.24 \text{ ms}^{-1}$ .

A more plausible assumption is that the boundary in the free atmosphere would be dominant. This favours the maintenance of the absolute wind profile, and it is the relative profile that is now shifted:

$$\vec{u}_{\text{abs}}(z) \sim \vec{u}_{\text{nocur}}(z), \quad \vec{u}_{\text{rel}}(z) \sim \vec{u}_{\text{nocur}}(z) - \vec{u}_{\text{oc}}. \quad (9)$$

Since  $\vec{u}_{\text{rel}}$  has changed, and thus according to (6) the stress, this solution does not exactly satisfy (2, 3, 5), and the entire profile has to be reintegrated. For the example presented in Figure 1, assume that the boundary condition is unaltered at a height of 100 m. When, for the sake of simplicity it is assumed that the constant stress approximation could still be used at this height, reintegration of (1-3), together with condition  $u_{\text{abs}}(100 \text{ m}) = u_{\text{nocur}}(100 \text{ m})$ , leads to the red dashed profile. As a result, surface stress and roughness length are somewhat reduced ( $u_*$  from  $0.30 \text{ ms}^{-1}$  to  $0.27 \text{ ms}^{-1}$ , and  $z_0$  from  $0.17 \text{ mm}$  to  $0.14 \text{ mm}$ ). The absolute wind speed has increased from  $8.24 \text{ ms}^{-1}$  to  $8.44 \text{ ms}^{-1}$ , rather than to remain unchanged as (9) suggested. In this case, it appears that the stress goes down while the (absolute) wind speed goes up. This can be explained simply by the picture that the movement of the surface in the direction of the flow decreases the friction (stress) at the surface, which therefore slows down the flow near the surface to a lesser extent. The change in relative wind speed is  $0.80 \text{ ms}^{-1}$ , rather than what was expected by (9) ( $1.00 \text{ ms}^{-1}$ ).

In practice both the boundary conditions at the surface and higher up in the atmosphere will play a role. The example of Figure 1 may be over simplistic, but it does illustrate that a moving ocean current will affect

surface stress, and therefore the entire wind profile. At 10-metre height, absolute wind speed is expected to increase somewhat for an ocean current in the direction of the flow ('less friction'), and to decrease somewhat when the current is opposite to the flow ('more friction'). As a result, assumption (9) will not be completely correct. Therefore the effect of ocean current on surface stress cannot be immediately guessed from operational ECMWF 10-metre wind in which no information on ocean current had been supplied to the boundary condition. Although in lowest approximation the assumption that absolute wind at 10-m height is unaffected by an ocean current may be reasonable, some fraction  $x$  of  $\vec{u}_{oc}$  will be absorbed in  $\vec{u}_{abs}(10\text{ m})$ , leaving a fraction  $1 - x$  for a change in relative wind, and thus the surface stress. Therefore, the effect of ocean current on surface stress may be smaller than one may expect at first sight. The simple example given above suggests a reduction in the order of 20%. Of course, only a proper integration of the model with inclusion of (1) can provide quantitative estimates.

### 3 The inclusion of ocean current in ocean wave forecasting

At ECMWF, ocean-surface wave forecasting is an integral part of the IFS. This is achieved by two-way coupling of the atmosphere model with a wave model (Janssen, 2004). The ocean-wave model is a derivative from WAM (Komen *et al.*, 1994), which is a third-generation model that provides an evolution of the wave spectrum  $F(\vec{k}, \vec{x}, t)$ . This quantity represents the energy density of ocean waves with wave vector  $\vec{k}$  within an area around position  $\vec{x}$  that is sufficiently large compared to the length of the waves themselves. The basic transport equation is given by:

$$\left\{ \frac{\partial}{\partial t} + (\vec{c}_g + \vec{u}_{oc}) \cdot \frac{\partial}{\partial \vec{x}} - \left( \frac{\partial}{\partial \vec{x}} \Omega \right) \cdot \frac{\partial}{\partial \vec{k}} \right\} \left( \frac{F}{\sigma} \right) = S_{in} + S_{nl} + S_{ds} + S_{bot}. \quad (10)$$

Here

$$\sigma(\vec{k}, \vec{x}) = \sqrt{g \|\vec{k}\| \tanh(\|\vec{k}\| d(\vec{x}))}, \quad \vec{c}_g = \frac{\partial}{\partial \vec{k}} \sigma \quad \text{and} \quad \Omega(\vec{k}, \vec{x}, t) = \sigma + \vec{k} \cdot \vec{u}_{oc} \quad (11)$$

are respectively the intrinsic frequency, group velocity and dispersion relation.  $d$  is the local water depth. This equation expresses that any change in wave action ( $F/\sigma$ ) is imposed by (in space) local sources and sinks, which are wave growth due to wind input  $S_{in}$ , non-linear interaction between waves  $S_{nl}$ , and dissipation due to white-capping  $S_{ds}$  and bottom friction  $S_{bot}$ . At ECMWF, an equation for  $F$  rather than  $F/\sigma$  is solved by an appropriate rewriting of (10). Details on the physical description and numerical implementation of the operational WAM model at ECMWF may be found in Part VII of the IFS-documentation (2006).

The wind input  $S_{in}$ , which is based on a formulation of Janssen (1991), describes the interface with the atmosphere. Wave growth due to wind mainly depends on the ratio between the component of friction velocity  $\vec{u}_*$  in wave propagation direction and phase speed, and some additional quantities such as air density and atmospheric stability. These quantities are provided by the atmospheric component. For historical reasons, the neutral wind at 10-metre height, rather than the friction velocity is passed to the wave model:

$$\vec{u}_n = \frac{\vec{u}_*}{\kappa} \ln\left(\frac{10 + z_0}{z_0}\right). \quad (12)$$

According to Janssen (1991), the ocean-wave spectrum influences the Charnock parameter  $\alpha_{ch}$ . This wave-age dependent quantity is passed back to the atmosphere, where it is used in (3) to update the sea-surface roughness length.

Regarding ocean currents, there are two contributions. First of all, the effect of the current on the wind profile, as described in the previous section, will affect the stress, and thus the neutral wind (12). This change should in principle be incorporated in the atmospheric component of the IFS.

The other contribution regards the advection term in the lhs of (10) and dispersion relation  $\Omega$  in (11). Due to a horizontally inhomogeneous ocean current field, wave refraction may occur, swell will deflect, and ocean waves can even be blocked or reflected. This intrinsic effect on ocean waves is in principle incorporated in the

Saturday 3 November 2007 00UTC Analysis t+ VT: 00UTC Surface: V velocity/U velocity  
 Saturday 3 November 2007 00UTC Analysis t+ VT: 00UTC Surface: \*\*U velocity  
 MERCATOR SURFACE CURRENTS from global PSY3V1 system

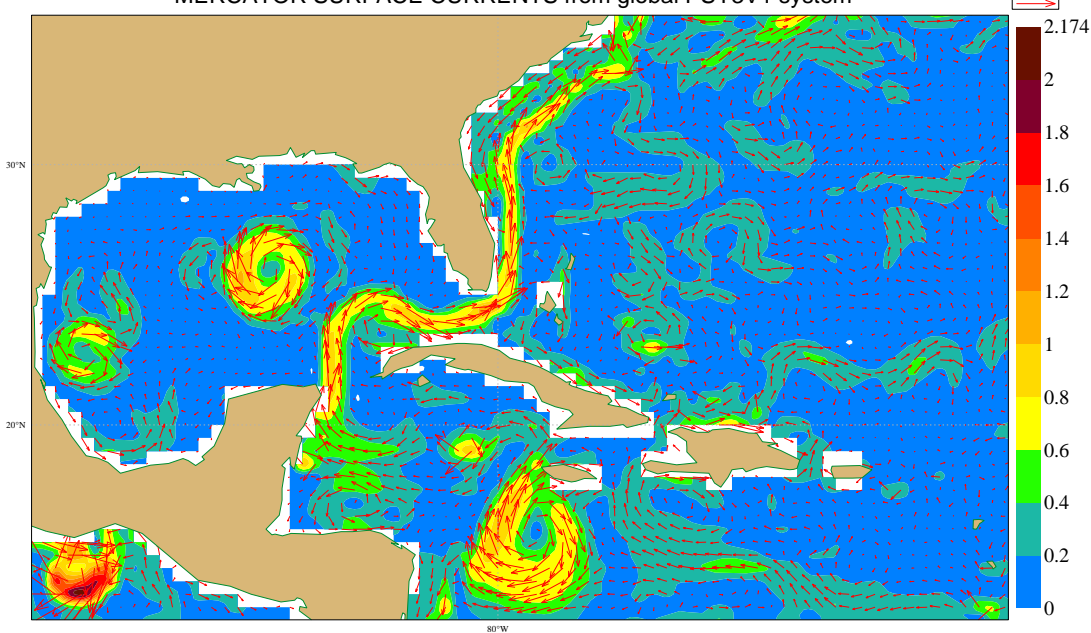


*Figure 2: An example of an ocean surface current field from the MERCATOR ocean model provided on a 0.5x0.5-degree grid for 3 October 2007. Arrows denote the direction, colors the strength of the ocean current. Courtesy of MERCATOR.*

standard formulation of the wave model. It should be noted that in the derivation of (10) it has been assumed that the ocean current does not depend on depth in the few tens of metres near the surface where they could influence the ocean waves.

## 4 An ocean-wave hindcast study

In this section some potential impact of ocean current on ocean-waves will be explored in a hindcast environment. In such a set-up, the wave model is forced by given ECMWF analysis fields. Any feedback from the waves on the atmosphere (via  $\alpha_{ch}$ ) is disregarded. Another simplification is that the detailed effect of ocean current on the atmosphere is not taken into consideration. It is assumed that the model absolute wind  $\vec{u}_{abs}$  is unaltered, and that the entire effect of the ocean current is absorbed in the relative current  $\vec{u}_{rel}$ . Therefore a separate set of atmospheric analyses fields does not have to be provided to incorporate the effect of ocean current on the wind forcing. Relation (9) applied to the neutral wind  $\vec{u}_n$  can be followed, instead. Although these assumptions may not appear to be perfectly justified, they do provide a simple but effective way to investigate the direct impact of ocean currents on ocean waves.

The question on the source for ocean current now arises. Requirements are a sufficient resolution on a global scale and a proper assimilation system, such that realistic features are resolved and well described. Examples would include a sharp definition of the Gulf stream, equatorial currents and counter-currents, and eddies. For the reason of consistency it is desirable that the ocean model from which the currents will originate has been forced with ECMWF (analysis) fluxes. Several candidates have been considered. One example is the TOPAZ3 system from NERSC (TOPAZ, 2007). It is based on the modified HYCOM ocean model with a resolution between 8-12 km. Its data assimilation embodies an Ensemble Kalman Filter using 100 members. Atmospheric forcing is from ECMWF. This model is only run in the Atlantic area. Although this system, therefore, is not suitable for conducting a global impact study, some experimentation has been performed for the high-resolution limited

area wave model that is run operationally at ECMWF for the North-Atlantic and Mediterranean. Results of these experiments, though, will not be reported in this document.

Another good candidate is the ocean model from [MERCATOR \(2007\)](#). This system involves the NEMO ocean model and is run on a horizontal resolution of 0.25 degrees on a global scale (disseminated products are only available at 0.5 degree). Daily analysis fields are available and are based on a Kalman-Seek method. Its atmospheric forcing also arises from ECMWF. The impact studies presented in this document will be based on this system. An example of a MERCATOR ocean surface current field is displayed in Figure 2. It shows a very well defined Gulf stream and Loop current.

Several hindcast experiments were conducted for the period between 17 March and 20 April 2008. All experiments involved the same setup of the global wave model, which was run at a slightly reduced horizontal resolution than the present operational resolution (0.5 degrees, rather than 0.36 degrees). The number of wave directions (24) and frequencies (30) was equal to the operational configuration.

A control experiment (to be called HCCTRL) involved a run without any current effects. A second experiment (denoted by HCWIND), only took the effect of the current on the wind input into account. This was, as discussed above, handled by the choice:

$$\vec{u}_n(\text{HCWIND}) = \vec{u}_n(\text{HCCTRL}) - \vec{u}_{oc}(\text{MERCATOR}). \quad (13)$$

A third experiment (named HCWADV) concentrated on the effect of currents on the wave advection. The forcing wind field was not adapted for this run, so  $\vec{u}_n(\text{HCWADV}) = \vec{u}_n(\text{HCCTRL})$ . A fourth experiment, including both the effect on wind forcing and wave advection was conducted as well. Since its results appeared more or less the sum of the results from the HCWIND and HCWADV runs, this experiment will not be further discussed.

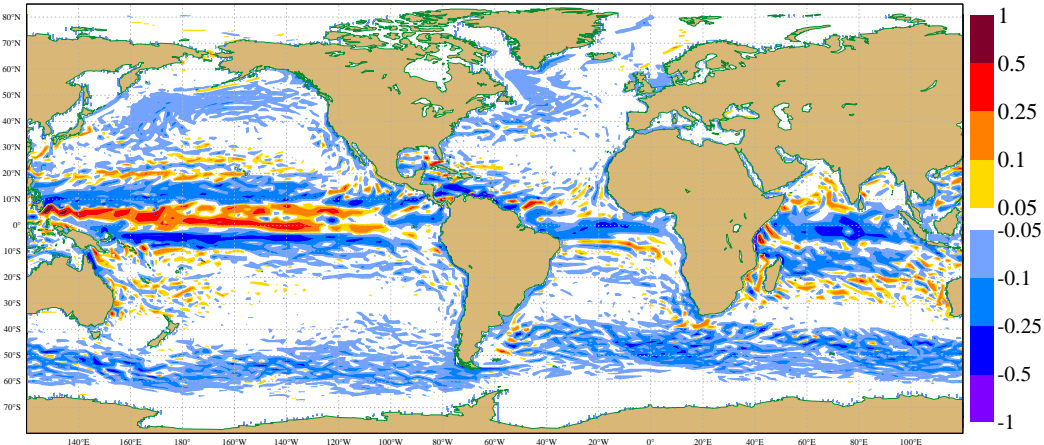
Some average results are summarized in Figure 3. Top panel shows the average difference in wind speed of applied wind forcing for the HCWIND experiment. Locally differences can exceed  $0.5 \text{ ms}^{-1}$ . On average, ocean currents are in the direction of the prevalent wind regime, so the relative wind speed has reduced. This is for instance the case along the Antarctic Circumpolar (ACC) Current and the North and South Equatorial currents. As a result, wave height has reduced in most areas around the globe, especially along the ACC. In the tropics, the Equatorial Counter Current enhances the relative wind speed. Here, wave height is increased. No clear effect from the Gulf Stream on wind speed emerges from the top panel of Figure 3. The reason for this is that the Gulf Stream current and the typical westerly winds are not aligned. When a vector difference would have been plotted a clear difference would have emerged. The effect on wave height in the region in the North Atlantic is a slight decrease in wave height. On average the response of wave height is modest. In isolated extreme cases, though, the effect may be up to 1 m. So although the average wave climate does not change too much, from the point of view of case by case ocean-wave forecasting there may be a significant effect.

The lower panel of Figure 3 shows the average response of wave height on the advection. The patterns for this HCWADV experiment are more large scale than the effect from the HCWIND run. It indicates that typically swell is affected, which acts on a long spatial scale. There are some more intense responses in the tropics, which are related to sharp gradients in the ocean current. The area East of the Philippines, for instance, indicates a response to the New Guinea Coastal Current.

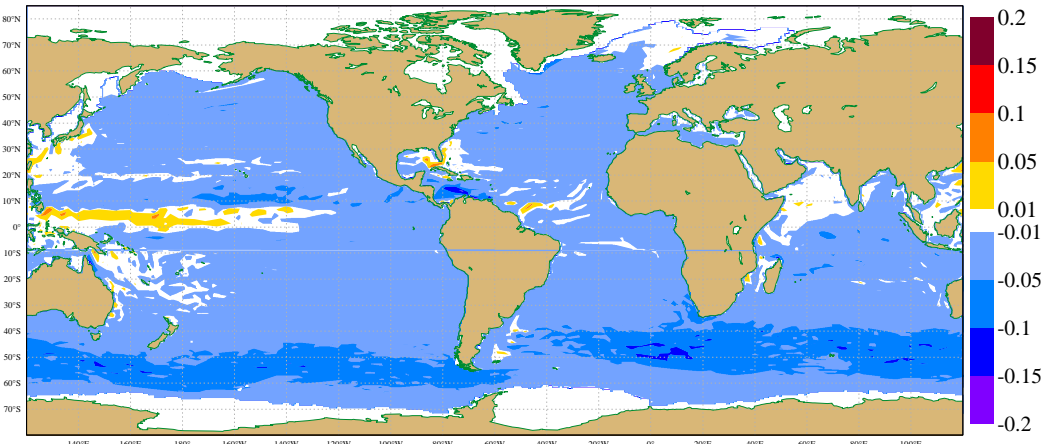
## 5 The inclusion of ocean current in the ECMWF 4D-Var assimilation system

The provision of the boundary condition (1) has been prepared in the ECMWF forecast model some time ago by Anton Beljaars. It would be straightforward to see the effect in a model integration. Starting from some initial condition and enforcing some ocean current field, like the MERCATOR field as used in the previous section, the difference with a standard control run that did not include currents can reveal the impact of such change. The initial condition for the model forecast arises from a data assimilation suite, where knowledge

Mean hindcast 10m neutral wind difference (HCWIND - HCNTRL)  
from 20080317 0Z to 20080420 18Z



Mean hindcast wave height difference (HCWIND - HCNTRL)  
from 20080317 0Z to 20080420 18Z



Mean hindcast wave height difference (HCWADV - HCNTRL)  
from 20080317 0Z to 20080420 18Z

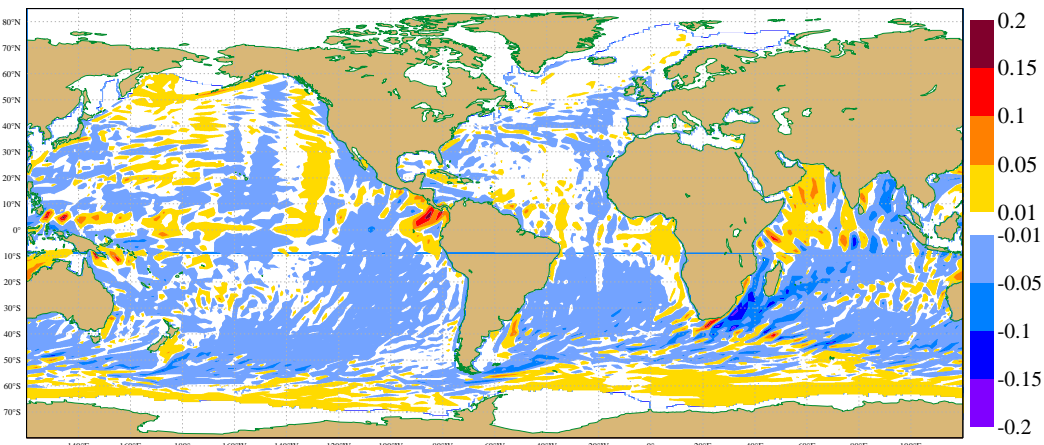


Figure 3: Average difference in forcing wind speed  $||\vec{u}_n(\text{HCNTRL}) - \vec{u}_{oc}(\text{MERCATOR})|| - ||\vec{u}_n(\text{HCNTRL})||$  (top panel) between HCWIND and HCNTRL, and average difference in significant wave height of HCWIND versus HCNTRL (middle panel), and HCWADV versus HCNTRL hindcast (lower panel). Units are  $\text{ms}^{-1}$  for wind speed and  $\text{m}$  for wave height.

from a previous forecast (also called the first guess or background) is mixed with new observational data. Such assimilation steps are essential, since without them, the forecast will soon loose any connection with reality. Since both the experiment and control would start from the same analysis, it takes some time for the effect of ocean currents to become visible. It would be better and more consistent to include the effect of ocean currents in the assimilation system as well. In this way the information of the ocean current will be able to cycle through the system. The impact is then to be assessed by the comparison of two assimilation suites, one with and one without ocean current. Many systems that use the ECMWF model as boundary condition are based on analysis fields, rather than forecast fields. An example are ocean models themselves. Both MERCATOR and TOPAZ, for instance, use ECMWF fluxes to drive their ocean models. Also from this point of view it is desirable to properly adapt the assimilation system, since ocean-current information that flows in from the model first-guess can be wiped out by surface observations when the effect of ocean current is neglected in the assimilation. The adaptation of the assimilation system would be a requirement when the usage of ocean currents is to become a part of the operational assimilation and forecast system at ECMWF.

ECMWF uses the method of incremental four-dimensional data assimilation (denoted by 4D-Var, [Courtier et al. \(1994\)](#)). For a given assimilation window, data is collected and compared to the model state via a cost function  $J$  that is to be minimized with respect to an increment  $\delta\mathbf{x}$  that corrects the background  $\mathbf{x}^b$  at the start of the assimilation window. Schematically,  $J$  is given by:

$$J(\delta\mathbf{x}) = J_b + J_o = \frac{1}{2}\delta\mathbf{x}^T \mathbf{B}^{-1} \delta\mathbf{x} + \frac{1}{2}(\mathbf{H}\delta\mathbf{x} - \mathbf{d})^T \mathbf{R}^{-1} (\mathbf{H}\delta\mathbf{x} - \mathbf{d}). \quad (14)$$

As stated above, the background is a short forecast from the previous analysis cycle. The  $J_b$  term expresses the confidence in this field via the background error covariance matrix  $\mathbf{B}$ . At the end of the minimization, the final increment  $\delta\mathbf{x}^a$  is added to the background  $\mathbf{x}^b$  to provide the analysis  $\mathbf{x}^a = \mathbf{x}^b + \delta\mathbf{x}^a$ .

The comparison between model and data is obtained via an observation operator  $H$ . It expresses what the value of observation should be according to the model. In 4D-Var the comparison between model and observation incorporates the timing of the observation as well. As a function of initial model state,  $H$  therefore includes a model integration from initial time to observation time. In (14),  $\mathbf{H}$  is a suitable linearization of  $H$  around the background, while the covariance matrix of observation errors  $\mathbf{R}$  expresses the accuracy of the observational network. The innovation vector  $\mathbf{d}$  is given by:

$$\mathbf{d} = \mathbf{y}^o - H(\mathbf{x}^b), \quad (15)$$

where the set of observations within the assimilation window is represented as a vector  $\mathbf{y}^o$ . The model integration started from the background over the entire assimilation window, that is required to calculate  $H$  for each observation in (15), is called the trajectory run (or outer loop). It is performed at the same resolution as the forecast model. Minimization (14), though, is performed at a reduced resolution (inner loop). This means that increments  $\delta\mathbf{x}$  and linearization  $\mathbf{H}$  are performed at a lower resolution, while innovation  $\mathbf{d}$  is calculated at full model resolution. The sequence of outer and inner loop is iterated a few times, in which the high resolution trajectory is readily updated. For the following discussion, though, the complication of inner and outer loops is not essential and its technical implications will not be further mentioned. A detailed description may be found in Part II of the [IFS-documentation \(2006\)](#).

The contribution of ocean current to the assimilation system is basically concentrated in the observation operator  $H$ . First of all, the trajectory run that involves the plain integration of model fields on model levels from the background over the assimilation window should satisfy boundary condition (1). This is straightforward, since that part is already available. Secondly, for observations that measure quantities near the sea surface the observation operator may have to be adapted. Such changes have to be handled separately, since the physics package that is used in  $H$  to calculate surface quantities from model variables at model levels, is not shared with the physics in the forecast model ([Cardinali et al., 1994](#)). For instance, the wind at an observation height  $z$  near or below the lowest model level  $z_L$  is estimated on the basis of a method by [Geleyn \(1988\)](#). Given the constant stress approximation no wind turning takes place and the wind vector is given by a simple reduction  $R$  from the wind vector at the lowest model level. Geleyn proposes the use of simplified gradient functions  $\Phi_M$

in (2) which then allows for the estimation of the value of  $R$  from available model quantities at lowest model level plus a knowledge of roughness length  $z_0$ . Since the method of Geleyn is based on a non-moving surface, it should now be applied to relative wind:

$$\vec{u}_{\text{rel}}(z_{\text{obs}}) = R \vec{u}_{\text{rel}}(z_L) = R (\vec{u}_L - \vec{u}_{\text{oc}}), \quad (16)$$

where it is realized that the model wind  $\vec{u}_L$  at lowest model level is defined in the absolute frame.

Let for a surface vector wind observation  $\vec{u}^{\text{obs}}$ , the observation operator  $H$  be denoted by  $\vec{u}^{\text{mod}}$ . Then the part of  $J_o$  in (14) that belongs to that specific observation is given by

$$J_o^{\text{surfwind}} = \frac{\|\vec{u}^{\text{mod}} - \vec{u}^{\text{obs}}\|^2}{\sigma_0^2}, \quad (17)$$

where  $\sigma_0$  determines the observation weight. It now depends on the nature of the surface wind observation how  $\vec{u}^{\text{mod}}$  is to be adapted. One source of wind observations that is used extensively at ECMWF is from scatterometer data ([Isaksen and Janssen \(2004\)](#), [Hersbach and Janssen \(2007\)](#)). A scatterometer is a microwave radar that emits pulses at well-defined frequency and polarization to the ocean surface. The magnitude of recorded backscatter is a measure for the strength of gravity-capillary surface waves. Since these waves respond to the local surface stress on a short time scale, they can be regarded as fully grown wind waves. Therefore, it is reasonable to suggest a one-to-one relation between backscatter and stress. Although different scatterometers may sense the surface at different frequencies (e.g., C-band or Ku-band), a unique relation between backscatter and stress should exist for each of them. For practical reasons, backscatter is usually related to 10-metre (neutral) wind, on the basis of an empirical geophysical model function. Examples are the QSCAT-1 model function for Ku-band (QuikSCAT, NSCAT, for an overview see [Chelton and Freilich \(2005\)](#)), and CMOD5 ([Hersbach et al., 2007](#)) for C-band (ERS and ASCAT). Observational evidence that scatterometer measure wind relative to a moving ocean surface was found by [Kelly et al. \(2001\)](#).

Another source of surface wind observations is from buoy and ship data. Moored buoys, such as the TAO array evidently measure wind with respect to an absolute frame. In summary, the adaptation of observation operator  $\vec{u}^{\text{mod}}$  depends on the nature of the observation as:

$$\text{scatterometer : } \vec{u}^{\text{mod}} = \vec{u}_{\text{rel}}(z_{10}) = R (\vec{u}_L - \vec{u}_{\text{oc}}), \quad (18)$$

$$\text{buoy/ship : } \vec{u}^{\text{mod}} = \vec{u}_{\text{abs}}(z_{\text{obs}}) = R \vec{u}_L + (1 - R) \vec{u}_{\text{oc}}. \quad (19)$$

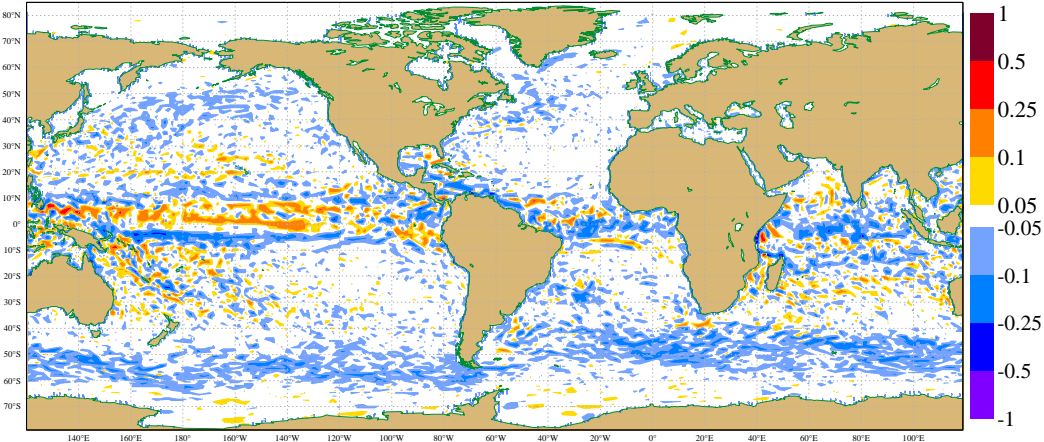
In the absence of ocean currents, (18) and (19) reduce to the observation operators for the operational assimilation system, i.e.,  $\vec{u}^{\text{mod}} = R \vec{u}_{\text{abs}}(z_L)$ . The observation operator for scatterometer data should strictly speaking act on equivalent neutral wind (12), or even better on  $\vec{u}_*$  (to account for sea-state effects in  $z_0$ ), rather than relative wind. Although the modification for neutral wind has been prepared (by a suitable redefinition of  $R$ ), this will not be discussed here. The lowest model level is in practice very close to 10 m, so  $R \approx 1$  in (18).

For buoy observations, adaptation (19) tries to hold on absolute wind. Many buoys measure wind at a height of 4 or 5 m, so  $R < 1$ . Relation (19) then illustrates that ocean currents can have an effect on an observation operator for wind measured in a fixed frame. In case model wind and ocean current are not aligned the observation operator will involve a change in wind direction. In practice though, the effect will be small. For the example given in Figure 1, e.g.,  $R = 0.92$  so nearly unity.

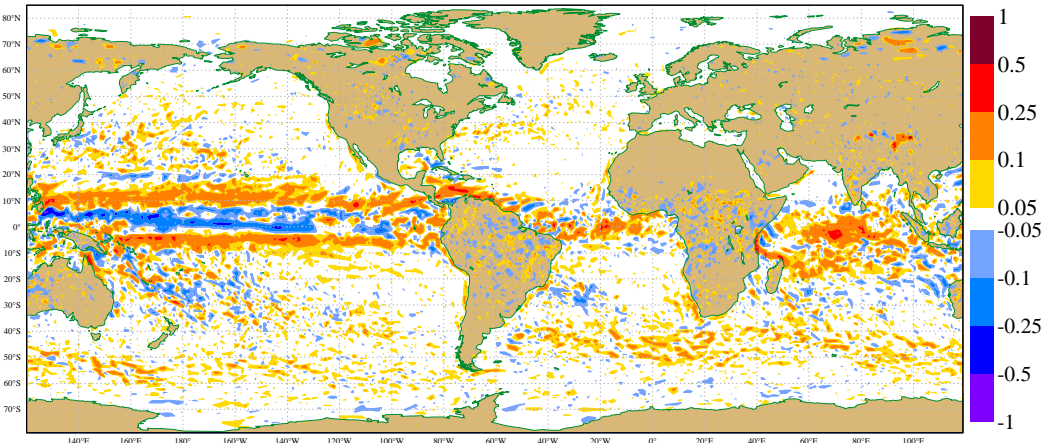
## 6 A data assimilation impact study

This section will present some results of an impact study within a data assimilation environment. In contrast to the hindcast study as discussed in Section 4, the ECMWF analysis winds that force the ocean-wave model are now subject to changes induced by the ocean currents, rather than being prescribed. In the final 4D-Var trajectory, wave data (such as altimeter wave height and SAR wave spectra) are assimilated and waves and

Mean analysed 10m neutral wind speed difference (DAWIND - DACNTR)  
from 20080317 0Z to 20080420 18Z



Mean analysis difference in 10m wind speed: DAWIND - DACNTR  
from 20080317 to 20080420



Mean analysed wave height difference (DAWIND - DACNTR)  
from 20080317 0Z to 20080420 18Z

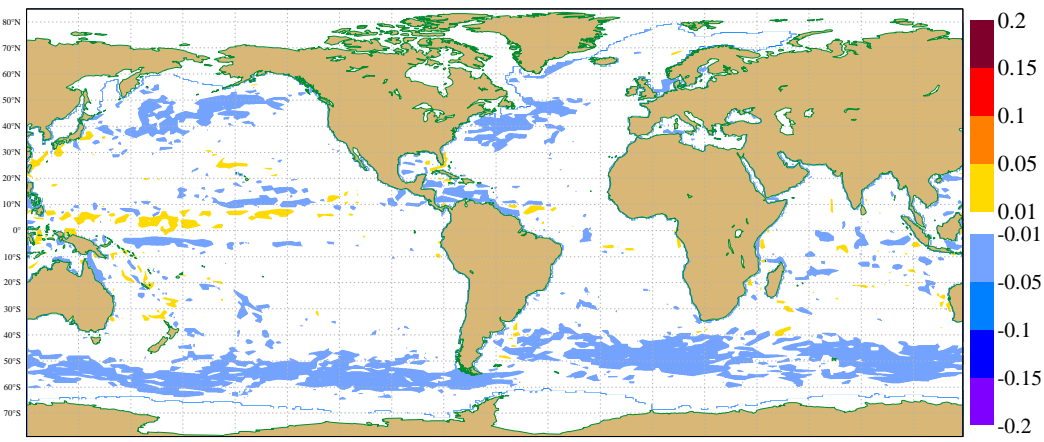


Figure 4: Difference in neutral wind speed (top panel, in  $\text{ms}^{-1}$ ), 10-metre absolute wind (middle panel, in  $\text{ms}^{-1}$ ) and significant wave height (lower panel, in m) between the DAWIND and DACNTR experiment averaged over the period 17 March to 20 April 2008.

atmosphere are two-way coupled. In an assimilation experiment information that is ingested in one cycle is propagated forward into the next cycle. It may be clear that this setup provides a more consistent frame work.

The adaptation of the assimilation system as described in the previous section was prepared. The observation operator (18, 19) was adapted. Regarding linearization (i.e.  $\mathbf{H}$  in minimization 14), associated tangent-linear and adjoint code was updated. An infrastructure for the inclusion of an ocean current from an external source was developed in a way that is similar to the ingestion of sea-surface temperature and sea-ice fraction at ECMWF. Since boundary condition (1) is respected in both the trajectory of 4D-Var and in the short-forecast run that connects subsequent analysis cycles, the full effect of ocean current is incorporated in the neutral wind (12). It is, therefore to be passed on directly to the ocean-wave model without any further corrections.

Two data assimilation experiments were conducted, a control (DACNTR) without, and an experiment (DAWIND) with the inclusion of ocean currents. In the latter experiment only the effect on the wind forcing (via the neutral wind from the adapted atmosphere) was taken into account. For technical reasons (that have meanwhile been resolved) it was not possible at the time to conduct a third experiment that includes the effect on wave advection.

The data assimilation experiments were performed for the same period as the hindcast study of Section 4 (17 March to 20 April 2008). For the DAWIND experiment, the same ocean current fields from [MERCATOR \(2007\)](#) were used. The resolution of the wave model was again 55 km in the horizontal, and 24 directions times 30 frequencies in wave-vector space. The horizontal resolution of the atmospheric model was reduced compared to the ECMWF operational system, i.e., T511, rather than T799 in spectral space, which corresponds to 40 km versus 25 km. The number of vertical levels was the same (91). The assimilation window was, like the operational suite, 12 hours, although experiments were not run in early-delivery mode (see Chapter II, [IFS-documentation \(2006\)](#)). For each day, a 10-day forecast was started from the analysis centred around 00UTC. The impact on these forecasts will not be discussed here, though.

The top panel of Figure 4 displays the average change in neutral wind speed (12) at analysis time. The effect appears to be significantly smaller than what was assumed in the hindcast study (top panel of Figure 3). Only about half of the effect of the ocean current is absorbed by the relative wind  $\vec{u}_{\text{rel}}$  (6), which, apart from stability effects is closely related to the neutral wind (12). The remaining 50% is shifted into a change in the absolute wind. This is shown by the middle panel of Figure 4. Where ocean current and wind are aligned, absolute wind in general increases (like displayed in Figure 1), where ocean current and wind are opposed absolute wind speed decreases. This seems especially to be an issue in the tropics. Hence, it appears that the assumption (9) that absolute wind can be regarded as nearly unaffected, on which the hindcast runs were based, is not justified. In line with a reduced effect on wind forcing, the response of the ocean-wave model is smaller as well. The lower panel of Figure 4 shows the impact in significant wave height for the DAWIND experiment, which is indeed much smaller than the impact in the HCWIND hindcast (middle panel of Figure 3).

## 7 Discussion

The reduced impact on the relative and neutral wind, due to the response of the absolute wind to an applied ocean current can originate from several effects. A first argument is along the lines of the simple example presented in Section 2 and Figure 1. It was shown there, that strictly speaking assumption (9) does not provide a valid solution. Due to a lower (enhanced) stress in case ocean current is aligned with (opposed to) the surface wind, the friction of the boundary layer with the ocean surface is enhanced (reduced) which, given more or less unaltered geostrophic conditions in the free atmosphere, will result in higher (lower) surface wind. For the example of Figure 1, where the original blue profile was slightly shifted (red profile), the effect was guessed to be 20%. Boundary condition (1) acts in both the 4D-Var trajectory and the short forecasts in between assimilation cycles. Therefore this effect is present in both the assimilation and forecast.

A second factor behind the reduced effect on relative wind may originate from the adapted assimilation system.

Since scatterometer data now act on relative model wind, the assimilation system will try to hold on the same values for stress at observed locations for the DAWIND and DACNTR experiment. For the example in Figure 1, the assimilation system would favour the situation of shifting the original blue profile (DACNTR) to the green curve (DAWIND), i.e., for a 100% shift of the ocean current into the absolute wind. Although at ECMWF scatterometer data is ingested in most areas within a 6-hour time window, the adapted observation operator will compete with other observations in which no adaptations were required. Among other reasons, this will limit the effect from scatterometer data. At first thought, it might be contradictory that the proper treatment of scatterometer data limits the impact. One should, however, realize, that the reason for this is not related to the experiment that includes ocean current (DAWIND), but due to an incorrect assimilation of scatterometer data as absolute wind in the DACNTR experiment. For this reason, to a limited extent, operational ECMWF surface wind may represent wind in a relative frame rather than in an absolute frame.

As mentioned, the work presented in this document is preliminary. Sofar, only a first assessment is being made in the basic understanding of the effect of an ocean current on the ECMWF assimilation and forecast system. In the next step, impact on forecast skill is to be taken seriously. The issue could be raised to what level of accuracy ocean currents are to be, and can be provided. A comparison between [MERCATOR \(2007\)](#) and [TOPAZ \(2007\)](#) showed that although both ocean models contain similar main structures (tropical currents and counter-currents, Gulf Stream, Kuroshio Extension, etc.), differences in the resolved Eddies are noted. Possibly some averaging may have to be performed to filter out uncertain features. Also, it may be queried to what level it is justified to keep the supplied currents constant during a 10-day integration. For extreme and rapidly moving systems, such as tropical cyclones, a response of the ocean current on an evolving atmosphere, may require a two-way coupled ocean-atmosphere system from the start of the forecast.

## Acknowledgements

We would like to thank Anton Beljaars, Peter Janssen, Tim Stockdale, Magdalena Alonso Balmaseda and Frederic Vitart for their useful discussions and suggestions. The work presented in this document was partly funded by ESRIN (Project Ref. 22025/08/I-EC). We would like to thank MERCATOR OCEAN for the kind provision of their ocean-current data.

## References

- Cardinali, C., Andersson, E., Viterbo, P., Thépaut, J.-N. and Vasiljevic, D. (1994). Use of conventional surface observations in three-dimensional variational data assimilation. *ECMWF Tech. Memo. No. 205*.
- Chelton, D. B. and Freilich, M. H. (2005). Scatterometer-based assessment of 10-m wind analyses from the operational ecmwf and ncep numerical weather prediction models. *Mon. Wea. Rev.*, **133**, 409–429.
- Courtier, P., Thépaut, J.-N. and Hollingsworth, A. (1994). A strategy for operational implementation of 4D-Var, using an incremental approach. *Q. J. R. Meteorol. Soc.*, **120**, 1367–1388.
- Geleyn, J.-F. (1988). Interpolation of wind, temperature and humidity values from the model levels to the height of measurement. *Tellus*, **40**, 347–351.
- Hersbach, H. and Janssen, P. (2007). Preparation for assimilation of surface-wind data from ascat at ecmwf. *Ecmwf research department memorandum*, ECMWF, Shinfield Park, Reading, available on request, [R60.9/HH/0750].
- Hersbach, H., Stoffelen, A. and de, S. H. (2007). An improved c-band scatterometer ocean geophysical model function: Cmod5. *J. Geophys. Res.*, **112** (C3), doi:10.1029/2006JC003743.
- IFS-documentation (2006). edited by Bob Riddaway. *available from www.ecmwf.int/research/ifsdocs/*.

- Isaksen, L. and Janssen, P. A. E. M. (2004). Impact of ERS scatterometer winds in ECMWF's assimilation. *Q. J. R. Meteorol. Soc.*, **130**, 1793–1814.
- Janssen, P. A. E. M. (1991). Quasi-linear theory of wind wave generation applied to wave forecasting. *J. Phys. Oceanogr.*, **21**, 1631–1642.
- Janssen, P. A. E. M. (2004). *The Interaction of Ocean Waves and Wind*. Cambridge University Press.
- Kelly, A. K., Dickinson, S., McPhaden, J. and Johnson, G. C. (2001). Ocean currents evident in satellite wind data. *Geophys. Re. Lett.*, **28**, 2,469–2,472.
- Komen, G. J., Cavalieri, L., Donelan, M., Hasselmann, K., Hasselmann, S. and Janssen, P. A. E. M. (1994). *Dynamics and Modelling of Ocean Waves*. Cambridge University Press.
- MERCATOR (2007). The Mercator ocean model. [www.mercator-ocean.fr](http://www.mercator-ocean.fr).
- TOPAZ (2007). The TOPAZ ocean model. [www.topaz.nerc.no](http://www.topaz.nerc.no).
- Vitart, F., Bonet, A., Balmaseda, M., Balsamo, G., Bidlot, J.-R., Buizza, R., Fuentes, M., Hofstadler, A., Molteni, F. and Palmer, T. (2008). Merging vareps with the monthly forecasting system: a first step towards seamless prediction. *ECMWF Newsletter*, **115**, 35–44.